

1 **Comparing Reservoir and Outcrop Specimens for Mixed Mode**
2 **I–II Fracture Toughness of a Limestone Rock Formation at**
3 **Various Conditions**

4 By

5 **N. Al-Shayea**

6 Department of Civil Engineering, King Fahd University of Petroleum and Minerals,
7 Dhahran, Saudi Arabia

8 Received September 14, 2000; accepted February 22, 2002
9 Published online ■ © Springer-Verlag 2002

10 **Summary**

11 A fracture toughness study was conducted on a limestone rock formation from a petroleum
12 reservoir in Saudi Arabia, and results were compared with those for outcrop specimens
13 from the same geological formation. The objective was to investigate the possibility of using
14 outcrop specimens to estimate the fracture toughness behavior of reservoir rock at *in-situ*
15 conditions of temperature and confining pressure. The study was made on reservoir speci-
16 mens from a depth of about 3.5 km, at both ambient and reservoir conditions. Mixed mode
17 I–II fracture toughness at reservoir conditions of high temperature and confining pressure
18 was studied using straight notched Brazilian disk (SNBD) specimens under diametrical
19 compression. Tests were conducted at ambient conditions, at an effective confining pressure
20 (σ_3) of 28 MPa (4000 psi), and at a temperature of 116 °C. The results showed a substantial
21 increase in fracture toughness under confining pressure. Under $\sigma_3 = 28$ MPa, the pure
22 mode-I fracture toughness (K_{IC}), increased by a factor of about 3.2, and the pure mode-II
23 fracture toughness (K_{IIC}) increased by a factor of 4.4, compared to those under ambient
24 conditions. On the other hand, K_{IC} at 116 °C was only 25% more than that at ambient
25 conditions. These results were compared with recent results for outcrop specimens from the
26 same geological formation. The results reveal that outcrop specimens can be successfully
27 used to predict the fracture behavior of reservoir specimens at *in-situ* conditions, in spite of
28 some differences at ambient conditions. Additionally, fracture toughness envelopes were
29 obtained for reservoir specimens at ambient and high pressure conditions, in both positive
30 and negative regions.

31 **Notations**

32 β	orientation angle of the notch with the direction of loading
33 σ_3	effective confining pressure (MPa)
34 θ	incident angle of x-rays on atomic plane
35 a	half crack length

1	B	thickness of the disk
2	FPZ	fracture process zone
3	K_I	Mode-I stress intensity factor
4	K_{IC}	pure Mode-I stress intensity factor
5	$K_{IC(\sigma_3)}$	pure Mode-I fracture toughness (MPa m ^{1/2}) under any confining pressure (σ_3)
6	$K_{IC(\text{field})}$	pure Mode-I fracture toughness (MPa m ^{1/2}) at field conditions
7	$K_{IC(T)}$	pure Mode-I fracture toughness (MPa m ^{1/2}) at any temperature (T)
8	K_{II}	Mode-II stress intensity factor
9	K_{IIC}	pure Mode-II stress intensity factor
10	LEFM	linear elastic fracture mechanics
11	M.Y.B.P.	million year before present
12	N_I	normalized Mode-I stress intensity factor for notched Brazilian disk
13	N_{II}	normalized Mode-II stress intensity factor for notched Brazilian disk
14	P	compressive load at failure
15	R	radius of the Brazilian disk
16	R^2	coefficient of determination
17	SNBD	straight-notched Brazilian disk
18	T	temperature

19

1. Introduction

20 Studying the fracture toughness of rocks at elevated temperatures and confining
 21 pressures is valuable for a number of practical situations such as hydraulic frac-
 22 turing used to enhance oil and gas recovery from a reservoir, and the disposal or
 23 safe storage of radioactive waste in underground cavities. Hydraulic fracturing is a
 24 well-known technique used to create fractures in deep-seated rock formations in
 25 order to enhance oil or gas recovery from a reservoir of low permeability. The ease
 26 of creating fractures is strongly influenced by the rock fracture toughness, which is
 27 a measure of the material's resistance against crack initiation and propagation.
 28 The study of rock fracture toughness under *in-situ* conditions (i.e. high temper-
 29 atures and confining pressures) becomes an important input for designing various
 30 aspects of the hydro-fracturing process (Sih and Liebowitz, 1968; Abou-Sayed,
 31 1978; Abe et al., 1979; Rummel and Winter, 1982).

32 Usually, the depth of hydraulic fracturing operation is in the range of 1 to 4
 33 km. The fracture toughness at that depth (i.e. at *in-situ* conditions) is required in
 34 order to predict a realistic value for hydro-fracturing pressure. Due to the high
 35 cost of field testing, laboratory testing is the only viable alternative to determine
 36 the fracture toughness of a rock formation at simulated reservoir conditions of
 37 temperature and pressure using small core specimens. Nevertheless, the limited
 38 availability of core specimens from a deep-seated formation, the high cost involved
 39 in most situations, and their poor quality in some cases are still big hurdles in a
 40 comprehensive experimental investigation. However, the problem may be solved if
 41 the outcrop specimens obtained from the same geological formation as that of the
 42 reservoir can be used for the fracture toughness evaluation.

43 The literature shows that little attention has been paid to the effect of specimen
 44 origin on fracture toughness. A comparison between the properties of outcrop and
 45 reservoir rocks from the same formation need to be correlated. This correlation
 46 has significant practical implications, since it allows the use of outcrop rock speci-

1 mens to determine the properties of reservoirs rocks of the same formation. The
2 outcrop rock specimens are many orders of magnitude less expensive than reser-
3 voir ones.

4 This study investigates the effect of specimen origin on Mode-I and mixed
5 Mode I–II fracture toughness by comparing two sets of rock specimens from the
6 same geological formation, one collected from an outcrop in the Central Province
7 of Saudi Arabia and the other from a gas reservoir in the Eastern Province. A
8 straight-notched Brazilian disk (SNBD) specimen type was used (Fig. 1), because
9 it is very convenient and eminently suitable for fracture toughness determination
10 in mixed Mode I–II conditions. Tests were made at ambient and *in-situ* conditions
11 of temperature and confining pressure.

12 2. Literature Review

13 Based on the loading type, there are three basic crack propagation modes in a
14 fracture process, namely: Mode I (extension, opening), Mode II (shear, sliding),
15 and Mode III (shear, tearing). Any combination of these modes can occur as a
16 mixed-mode. Most, if not all, studies in the past have focused on fracture tough-
17 ness determination under confining pressures only for Mode-I failure conditions
18 (Perkins and Krech, 1966; Schmidt and Huddle, 1977; Muller, 1986; and Vasar-
19 helyi, 1997). Nevertheless, due to randomly oriented cracks in rocks and/or in-situ
20 stress conditions, cracks tend to propagate under the influence of a combined
21 action of the basic failure modes called mixed mode (Whittaker et al., 1992; and
22 Lim et al., 1994-a). In the case of rocks, the combination of Mode-I and Mode-II
23 (mixed Mode I–II) failure is more common. Therefore, consideration of mixed
24 Mode I–II loading in addition to pure Mode-I becomes important in fracture
25 toughness investigation.

26 Rock specimens should be relatively small in size, requiring minimum machin-
27 ing for sample preparation, particularly when specimens are obtained from large
28 depths (i.e. reservoirs). A centrally notched disk type specimen under diametrical
29 compression has been extensively used in the past for fracture toughness studies of
30 brittle materials including rocks under ambient conditions (Awaji and Sato, 1978;
31 Sanchez, 1979; Atkinson et al., 1982; Shetty et al., 1986; Fowell and Xu, 1994;
32 Lim et al., 1994-a; and Krishnan et al., 1998). However, the available data for
33 mixed Mode I–II fracture toughness under confining pressures and high tempera-
34 ture is limited.

35 The literature shows that most of the studies related to fracture toughness under
36 confining pressures have been limited to Mode-I conditions. Moreover, specimen
37 types other than the Brazilian disk have been used in these investigations. Due to
38 the fact that actual crack propagation in rock is caused by a force field of mixed
39 Mode I–II, and since the only way to obtain samples from a deep-seated rock
40 formation such as a reservoir is by coring cylindrical specimens, it is a matter of
41 potential interest to investigate the fracture toughness for mixed Mode I–II load-
42 ing conditions by using disk type specimens (Figure 1). This specimen geometry
43 was chosen in this study because it allows testing under Mode-I, Mode-II, and

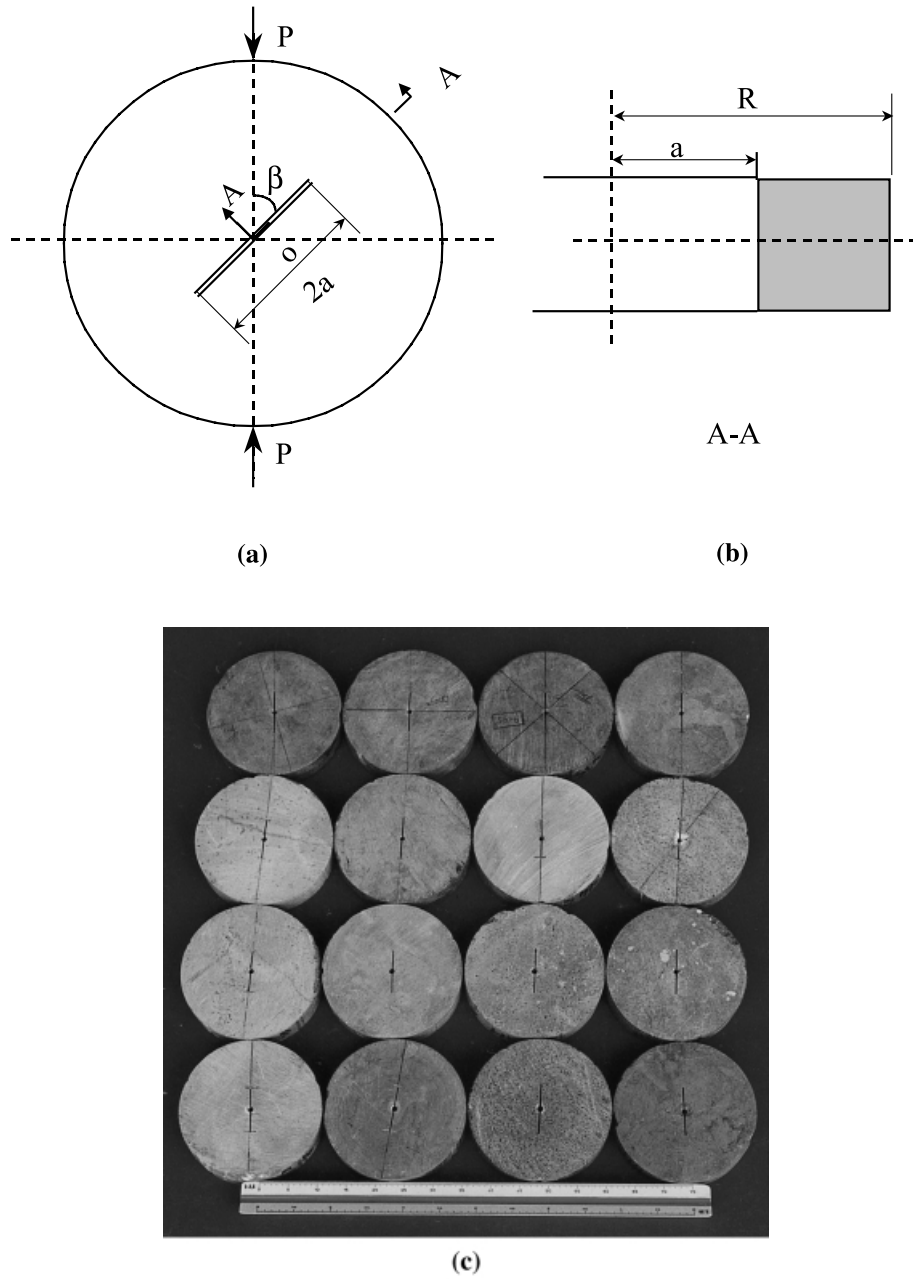


Fig. 1. Notched Brazilian disk specimen under diametrical compression (a), cross sectional area through the straight notch (b), and samples of Brazilian disk specimens with straight notches (c)

1 mixed-Mode I–II loading conditions using the same specimen configuration and
2 the same experimental setup. Variations in specimen geometry and testing setup
3 were thus eliminated. By changing the orientation angle of the notch with respect
4 to the direction of loading (β), any loading condition can be obtained: pure
5 Mode-I ($\beta = 0^\circ$), pure Mode-II ($\beta \approx 30^\circ$), or mixed-Mode I–II.

6 Usually, the fracture toughness of rock is determined at ambient conditions
7 (at room temperature and atmospheric pressure). However, under varying temper-
8 atures and confining pressures, the measured fracture toughness has been shown to
9 vary. The fracture toughness behavior of a deep-seated rock formation requires
10 the testing to be conducted in a manner that simulates the *in-situ* conditions such
11 as temperature and confining pressure. Estimates based on field data have indi-
12 cated that representative hydrofracture toughness parameters are one to two orders
13 of magnitude higher than those determined at ambient conditions (Shlyapobersky,
14 1985). Several other studies on quarried rocks have showed a significant increase
15 in Mode-I fracture toughness with an increase in the confining pressure. The mea-
16 sured data shows a considerable scatter, but an increase which is roughly linear
17 with the confining pressure has been observed (Thallak et al., 1993).

18 Rock formations at larger depths have temperatures considerably higher than
19 the ambient, which is generally used during a laboratory study. A temperature
20 gradient of about $1^\circ\text{C}/30\text{ m}$ exists within the earth's crust (Mitchell, 1993). In the
21 past, little attention has been paid to the fracture toughness determination of rocks
22 with temperatures higher than the ambient. Hoagland et al. (1973) studied the ef-
23 fect of temperature on the fracture energy of Indiana limestone and Berea sand-
24 stone. They tested double cantilever beam specimens in splitting mode, at 22°C
25 and at 196°C . The results for both rocks indicated that the fracture energy at
26 196°C was considerably lower than that obtained at room temperature. Meredith
27 (1983) investigated the influence of high temperature on measured fracture tough-
28 ness (Mode I) using double torsion tests on Black gabbro, Westerly granite, and
29 single crystals of synthetic quartz at a temperature range between 20°C and 400°C .
30 His results showed that K_{IC} increased slightly with increasing temperature from
31 20°C to 100°C , while it steadily decreased with increasing temperature from
32 100°C to 400°C . This reduction may be mainly caused by the development of
33 microcracks resulting from the considerable tensile stress due to differential ther-
34 mal expansion between adjacent mineral grains in the rock sample. Atkinson et al.
35 (1982) obtained similar results for Westerly granite samples.

36 Although some studies have been carried out on the effect of temperature on
37 mode-I fracture toughness, little attention has so far been focused on mixed Mode
38 I–II. In the field, however, Mode-I may not be dominant, but Mode-II and in
39 particular mixed Mode I–II is frequently encountered (Whittaker et al., 1992).
40 Therefore, a study of mixed mode fracture toughness behavior at high temperature
41 is of significant importance in practice. Al-Shayea et al. (2000) investigated the
42 effect of confining pressure and high temperature on mixed Mode I–II fracture
43 toughness for a limestone rock. These rocks were obtained from the outcrop of the
44 same geological formation under consideration. Thus their results will be used in
45 this paper as a base for the comparison of the results of the reservoir rocks. This
46 comparison is of significant importance in practice.

3. Theoretical Background

3.1 Fracture Toughness

When a notched rock specimen is subjected to an externally applied load, stress concentrates in the vicinity of the crack tip. When this stress concentration reaches a critical value, failure occurs due to propagation of the preexisting crack. The fracture toughness is then calculated in terms of the stress intensity factor (SIF) using the failure load, notch size, and other geometrical parameters of the specimen. In this paper, a circular disk with a central straight notch under diametrical compression (Figure 1-a) was used to investigate fracture toughness. The following mathematical expressions, proposed by Atkinson et al. (1982), were used for the fracture toughness calculation:

$$K_{\text{I}} = \frac{P\sqrt{a}}{\sqrt{\pi RB}} N_{\text{I}} \quad (1)$$

$$K_{\text{II}} = \frac{P\sqrt{a}}{\sqrt{\pi RB}} N_{\text{II}}; \quad (2)$$

where:

K_{I} = Mode-I stress intensity factor;

K_{II} = Mode-II stress intensity factor;

R = radius of the Brazilian disk;

B = thickness of the disk;

P = compressive load at failure;

a = half crack length; and,

N_{I} and N_{II} are non-dimensional coefficients which depend on a/R and the orientation angle (β) of the notch with the direction of loading.

For linear elastic fracture mechanics (LEFM) to be applicable to the fracture toughness study, the fracture process zone (FPZ) should be as small as possible. This is achieved partly by limiting the crack size to a minimum but practical value (Schmidt, 1976), and partly by using specimens of relatively larger thickness (Barton, 1982). Based on that, the small crack approximation proposed by Atkinson et al. (1982) can be used to determine the values of N_{I} and N_{II} for half crack to radius ratio ($a/R \leq 0.3$), as follows:

$$N_{\text{I}} = 1 - 4 \sin^2 \beta + 4 \sin^2 \beta * (1 - 4 \cos^2 \beta) \left(\frac{a}{R}\right)^2 \quad (3)$$

$$N_{\text{II}} = \left[2 + (8 \cos^2 \beta - 5) \left(\frac{a}{R}\right)^2 \right] \sin 2\beta. \quad (4)$$

Although the above Eqs. (1) to (4) were derived for Brazilian disk tested at ambient conditions, they are also used in this paper for Brazilian disk tested at confining pressure. This is based on the fact that “*superposition of linear elastic fields*” applies to linear elastic stresses, Whittaker et al. (1992). For the case of testing at confining pressure, the total stress at the crack tip is the resultant of the

1 stresses generated by the confining pressure alone and those generated by the dia-
2 metrical compression alone. Since the confining pressure produces isotropic com-
3 pression, it causes the crack to close, and consequently the fracture toughness to
4 increase, i.e., it makes the rock tougher against fracture. Therefore, the fracture
5 of the confined rock is caused by the diametrical compression. This is analogous
6 to the case of the conventional triaxial test, in which the confining compression
7 increases the strength of the material, and the failure is caused by the deviatoric
8 stress.

9 3.2 Failure Theories

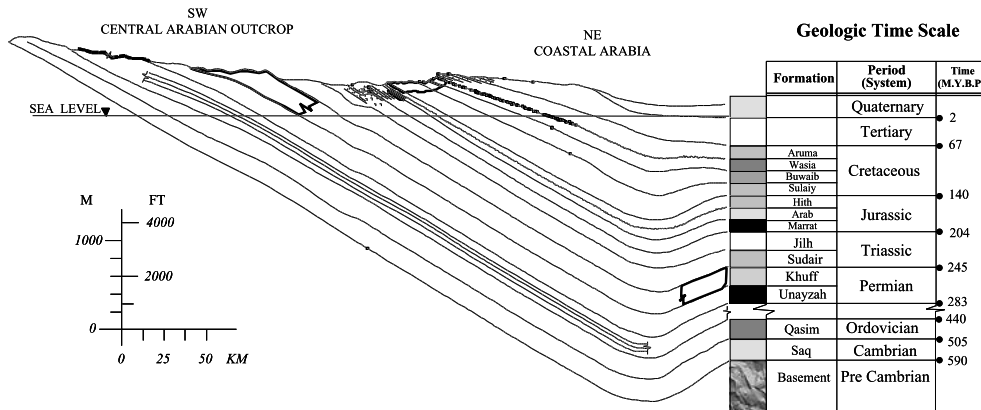
10 There are numerous failure criteria for crack initiation and propagation under
11 mixed Mode I–II loading condition. The most popular ones are: the maximum
12 tangential stress (σ) criterion, the maximum energy release rate (G) criterion, and
13 the minimum strain energy density (S) criterion. The available experimental data
14 shows that no distinct theoretical failure criterion is applicable to all cases. Also,
15 these criteria imply that K_{IC} is larger than K_{IIC} , while experimental data show the
16 opposite.

17 Moreover, due to the fact that the existing failure criteria were developed based
18 on the tensile loading rather than the compressive one, these criteria hold good
19 only in the positive region (crack opening) and cannot predict the fracture behav-
20 ior in the negative zone (crack opening). Many researchers have recommended
21 using empirical relations for practical applications. Huang and Wang (1985) and
22 Sun (1990) have used one of three empirical equations of straight line, ellipse,
23 and homogenous quadratic to fit the experimental fracture toughness data in the
24 (K_I/K_{IC}) - (K_{II}/K_{IIC}) plane. Also, an exponential relationship was used, Awaji and
25 Sato (1978), and Lim et al. (1994-b).

26 4. Geology and Rock Description

27 Rock samples were obtained from the “Khuff” formation in Saudi Arabia. Geo-
28 logically, the Khuff formation relates to the early Triassic to late Permian age (215
29 to 270 M.Y.B.P.). A general trend of the sedimentary rock formations in the region
30 is shown in Fig. 2a. The structural geology for this formation indicates that it
31 outcrops at various places in the Central Province of Saudi Arabia, with an alti-
32 tude reaching hundreds of meters above sea level (Fig. 2b), and it dips toward the
33 east to a depth of about two to four thousand meters below sea level in the Eastern
34 Province. The generalized lithology of the Khuff formation consists of layers of
35 limestone, claystone, dolomite, anhydrite, and sandstone.

36 The thickness of the Khuff formation increases basinward (from southwest to
37 northeast) from 450 to 975 m. In the Ghawar field, its thickness is 500 m, (Al-
38 Jalal, 1994). The carbonate and anhydrite sequence upward is subdivided into four
39 alternating anhydrite and carbonate intervals. From top to bottom, the anhydrite-
40 carbonate pairs are called Khuff A, B, C, and D. Powers et al. (1963) gave a gen-
41 eralized description of Lithology A as aphanitic-calcareous limestone, Lithology



a



b

Fig. 2. General trend of the sedimentary rock formations in Saudi Arabia (a), Khuff formation outcropping in Gassim area, sample collection location (b)

1 B as aphanitic limestone, Lithology C as dolomite and limestone, and Lithology D
2 as dolomite and shale.

3 Reservoir samples were collected from the Ghwar field, the largest oil reservoir
4 in the world producing oil and gas from multi-reservoir zones in the Khuff for-
5 mation. The reservoir samples were obtained by Saudi Aramco in the form of cores
6 from different depths and their lithology was found to vary. Moreover, many sam-

1 ples contained impurities such as anhydrite. To avoid sample inhomogeneity,
2 samples from one limestone lithology were selected for which much material
3 was available. The study was made on reservoir specimens from a depth of about
4 3.5 km.

5. Experimental Investigation

5.1 Rock Properties

7 Mineralogical composition plays an important role in the identification and clas-
8 sification of rock materials. Mineralogical compositions of the reservoir specimens
9 were determined by the X-ray diffraction (XRD) technique. The objective of this
10 analysis was to identify the mineral phases (chemical compounds) present in the
11 reservoir rock samples and to compare it with those of the outcrop samples, in
12 order to get an indication that both reservoir and outcrop rocks relate to the same
13 geological formation.

14 Some physical and mechanical properties were determined to characterize the
15 investigated limestone rock. Visual inspections were made. Dry density and spe-
16 cific gravity were determined according to ASTM D 1188 and ASTM D 854, re-
17 spectively (ASTM, 1993). The splitting tensile strength was found indirectly using
18 an uncracked Brazilian disk under diametrical compression, similar to ASTM D
19 3967.

5.2 Fracture Toughness

5.2.1 Sample Preparation

22 Reservoir cores were obtained from Saudi Aramco drilled from a depth of about
23 3.5 km. These cores have a diameter of about 100 mm. Cores were sliced into
24 circular disks using a high-speed circular saw. The thickness (B) of the sliced disks
25 was in the range of 20–24 mm. This thickness was decided according to the rec-
26 ommendations by Khan and Al-Shayea (2000). A straight notch was machined in
27 the center of the disks using a 0.25 mm diamond-impregnated wire saw. In the
28 notch making process, a hole was drilled in the center of the disk using a 3-mm
29 drill bit. The wire was passed through the drilled hole and the notch was machined.
30 This technique allows notches of any length to be made, and hence the difficulty
31 associated with machining small notches in Brazilian disks, as reported by Fowell
32 and Xu (1994), was overcome. A crack length of 29 mm was used (i.e., $a/R = 0.3$).
33 This ratio was decided according to the findings of Khan and Al-Shayea (2000).
34 Some of the notched disk specimens are shown in Fig. 1c.

35 For the testing under confining pressure, the entire disk surface was painted
36 with a glossy spray paint to avoid the penetration of pressurized oil during testing.
37 Also, the notch was sealed by adhesive tape on both sides, to prevent pressure
38 buildup inside the notch. A preliminary investigation showed the ability of the
39 paint to prevent oil infiltration. Two specimens were confined by pressurized oil
40 for a sufficient period of time; one was painted and the other was not. These two

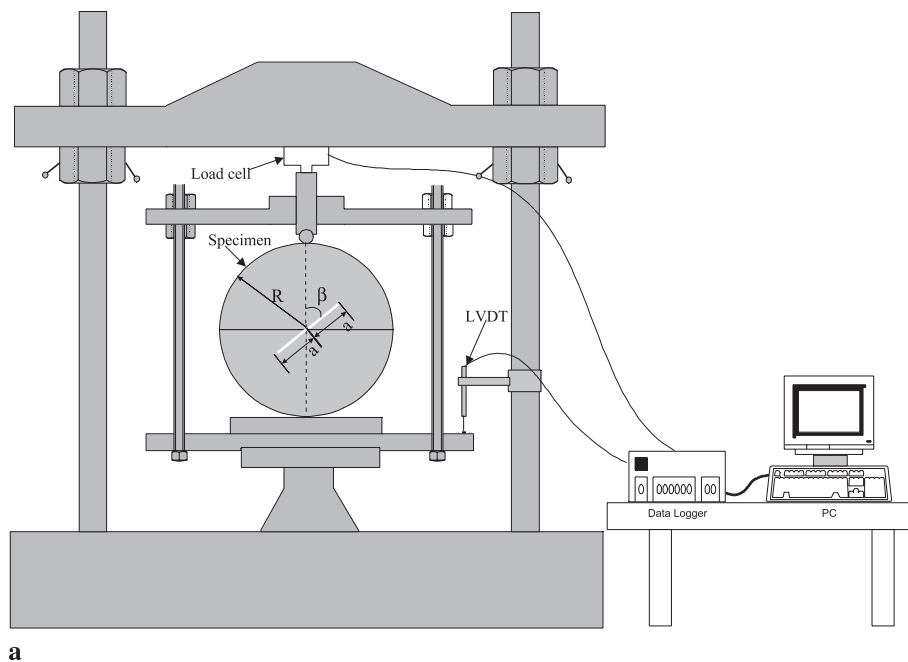
1 samples were taken out and then broken. The painted one showed no sign of oil
 2 infiltration, while the unpainted one showed an infiltration of oil to a depth of
 3 about 3 mm below surface. Additionally, the paint was thin enough not to affect
 4 the rock properties, especially the fracture toughness, since the notch itself was not
 5 spray-painted.

6 5.2.2 Testing at Ambient Conditions

7 A strain-controlled loading frame having a capacity of 100 kN was used for the
 8 load application with a strain rate of 0.08 mm/min, Fig. 3a. SNBD specimens with
 9 100 mm diameter and $a/R = 0.3$, were diametrically loaded. Reservoir specimens
 10 were tested with different values of the crack inclination angle (β) ranging from 0°
 11 to 75° with a 15° increment. The applied load and load-point displacement were
 12 acquired using a computerized data logger.

13 5.2.3 Testing at Reservoir Conditions

14 Al-Shayea et al. (2000) attempted to study the fracture toughness variation under
 15 the combined influence of temperature and pressure. Unfortunately, the applica-
 16 tion of confining pressure after heating of the sample was not successfully accom-
 17 plished. During the sample heating stage, the “O” rings in the triaxial chamber



a
Fig. 3. Schematic loading arrangement at ambient conditions, (a) Triaxial cell for testing under confining pressure, (b) Box for testing at high temperature

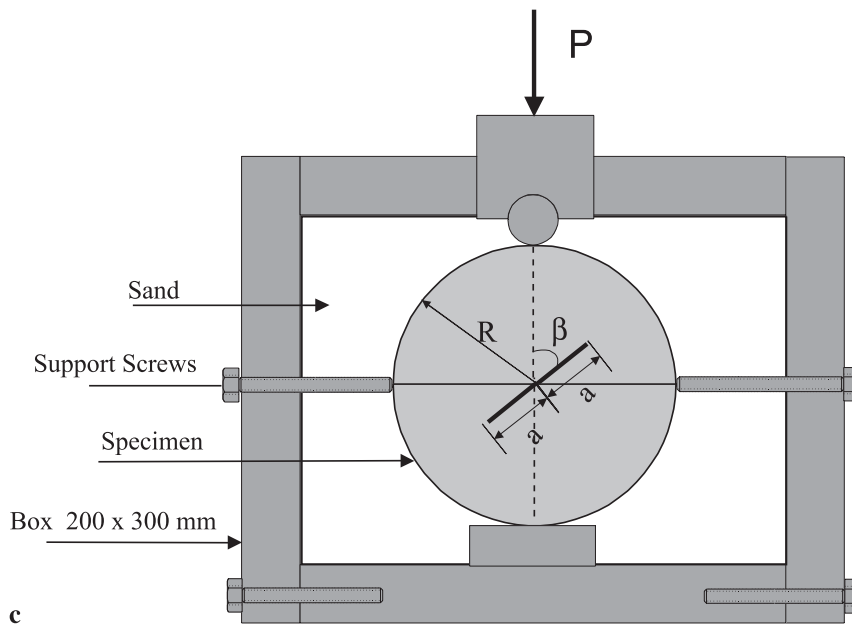
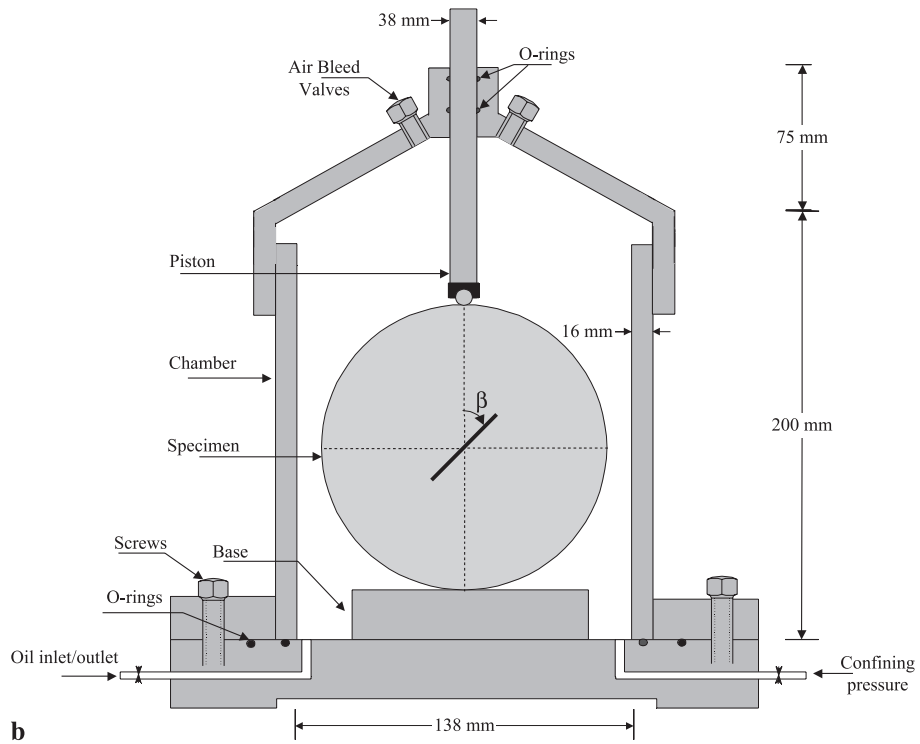


Fig. 3. (continued)

1 became soft and broke during the application of confining pressure, resulting in
2 leakage of oil from the cell. Many attempts were made to remedy the problem,
3 after which it was decided to decouple the application of temperature and confin-
4 ing pressure. In this study the effects of temperature and confining pressure on the
5 fracture toughness were also investigated independently.

6 5.2.3.1 Testing at Confining Pressure

7 Specimens were tested inside a triaxial cell made of stainless steel, manufactured
8 locally for this purpose, Fig. 3b. The cell was mounted into the apparatus shown
9 in Fig. 3a. The notched disk was placed, with the desired crack inclination to
10 loading direction, on a sample holder fixed to the base of the triaxial cell. Two
11 lateral screws on each side of the sample holder were made to gently touch the
12 sample to ensure its verticality. The disk was then fixed to the base of the sample
13 holder using quick-setting glue. A flat circular base snugly attached to a circular
14 rod was fixed on top of the specimen to precisely control the loading angle. The
15 triaxial chamber was tightly screwed to the base, and the whole assembly was
16 placed under the loading frame used for testing at ambient conditions. The
17 chamber was filled with a light oil, and confining pressure was applied by a hy-
18 draulic pump. A confining pressure (σ_3) of up to 28 MPa (4000 psi) was used in
19 this investigation, which is equal to the anticipated effective confining pressure in
20 the reservoir. The confined rock specimen was then diametrically loaded in com-
21 pression, while load and load-point displacement were recorded using a compu-
22 terized data acquisition system.

23 To study the variation in Mode-I fracture toughness from ambient to a con-
24 fining pressure of 28 MPa (4000 psi), reservoir specimens were tested under a σ_3 of
25 0 and 28 MPa only because of limited availability.

26 The effect of confining pressure on mixed Mode I–II fracture was investigated
27 using a σ_3 of 0 and 28 MPa. Reservoir specimens under these confining pressures
28 were tested with different values of the crack inclination angle (β) ranging from 0°
29 to 75° with an increment of 15°.

30 5.2.3.2 Testing at High Temperature

31 The effect of temperature on fracture toughness was investigated by testing speci-
32 mens inside a rectangular box fabricated from a heat and electrical insulation
33 material (Bakelite), Fig. 3c, to study the fracture toughness behavior at tem-
34 peratures simulating field conditions. The inside dimensions of the box were
35 200 mm × 300 mm × 200 mm height, and the wall thickness was 14 mm. Speci-
36 mens were placed inside the box at particular values of β , and precisely secured in
37 position with the help of two lateral screws. Then the box was filled with coarse
38 sand in a loose state, covered with a cap, and the whole assembly placed in an
39 oven for heating to the desired temperature. Due to the long time required for the
40 samples to reach a uniform temperature, only two samples per day could be tested.
41 After reaching the required temperature, the whole assembly was removed from

1 the oven, and the sample was diametrically compressed by the loading frame used
 2 for testing under ambient conditions. Load and load-point displacement was re-
 3 corded during testing.

4 A preliminary investigation was made in which the temperature was monitored
 5 directly on the specimen surface. The temperature was found to drop by only 2 °C
 6 in half an hour for the highest temperature of 116 °C. Since the time for each test
 7 was only five minutes, it was concluded that the slight drop (0.3 °C) in temperature
 8 was negligible. The samples were tested both in Mode-I and mixed Mode I–II
 9 loading conditions. For Mode-I, reservoir specimens were tested at temperatures
 10 of 27 °C and 116 °C (reservoir temperature) and only one sample for each condi-
 11 tion was tested. Due to the limited number of reservoir specimens, tests at tem-
 12 peratures of 27 °C and 116 °C were conducted only for pure Mode-I and pure
 13 Mode-II loading conditions.

14 6. Results and Discussion

15 6.1 Rock Properties

16 The mineralogical compositions of the reservoir rock, determined by XRD tech-
 17 nique, are shown in Fig. 4. XRD analysis conducted on the reservoir samples
 18 shows that their mineralogical compositions were nearly identical to those of the
 19 outcrop samples reported by Al-Shayea et al. (2000), which is pure limestone (99%
 20 CaCO₃). This indicates that these specimens are from the same geological forma-
 21 tion.

22 A visual inspection of the reservoir specimens showed that this limestone rock
 23 was a homogenous, muddy limestone. It was very tight and lacked any pores visible
 24 under a polarizing microscope, and therefore had a negligible porosity.

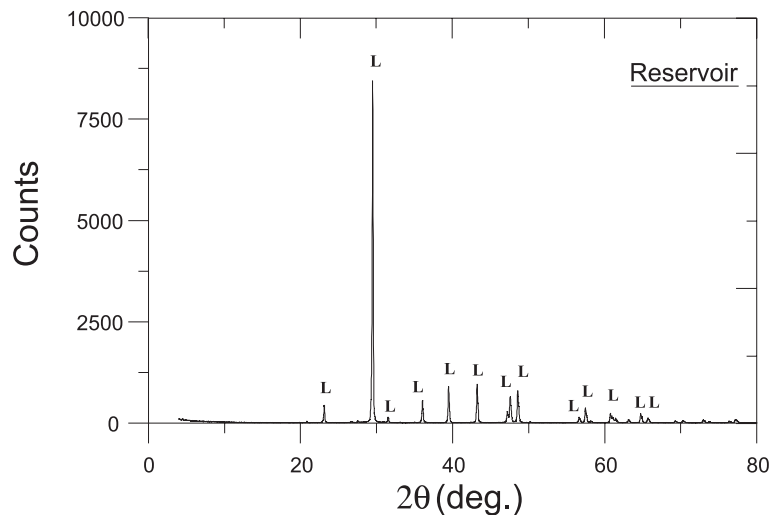


Fig. 4. XRD results for rock samples. The (L) indicates limestone

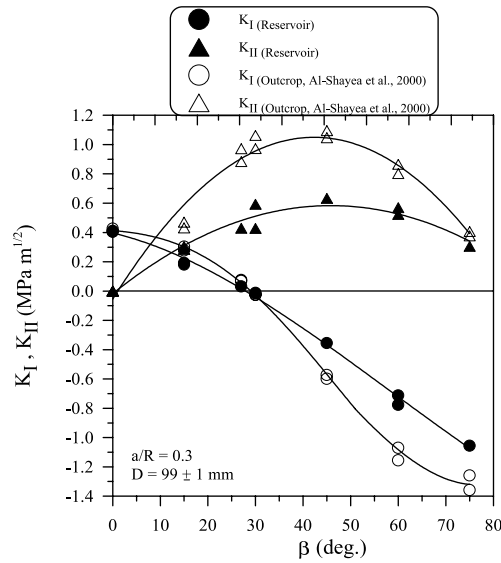


Fig. 5. Mixed Mode I–II fracture toughness for outcrop and reservoir specimens, at ambient conditions

1 The reservoir specimens were gray in color. Their physical properties included
 2 a dry density (ρ_d) of 2.664 gm/cm³ and a specific gravity (G_s) of 2.723. Using
 3 basic phase relationships, the void ratio ($e = [\{G_s\rho_w/\rho_d\} - 1]$) was 0.022, where
 4 ρ_w = density of water, and the porosity ($n = e/[1 + e]$) was 2.13%. The mechanical
 5 characteristics included $\sigma_t = 2.66$ MPa.

6

6.2 Ambient Conditions

7 Equations (1) to (4) were used to calculate the mixed Mode I–II fracture tough-
 8 ness for SNBD specimens made from reservoir samples at ambient conditions.
 9 Results are given in Fig. 5, which are also compared with those of the outcrop
 10 samples. The values of K_I and K_{II} for the reservoir samples are much lower than
 11 those of the outcrop samples. The pure Mode-I fracture toughness (K_{IC}) was 0.41
 12 and 0.42 for the reservoir and outcrop samples, respectively. The pure Mode-II
 13 fracture toughness (K_{IIC}) was 0.50 and 0.92 MPa m^{1/2} for the reservoir and
 14 outcrop samples, respectively. It is worth noting that K_{IIC} for reservoir specimens is
 15 much less than that of the outcrop specimens. The ratio of pure Mode-II to pure
 16 Mode-I (K_{IIC}/K_{IC}) was 1.22 and 2.19 for reservoir and outcrop, respectively.

17

6.3 Confining Pressure

18

6.3.1 Mode-I

19 Mode I fracture toughness was calculated using Eqs. (1) and (3) with $\beta = 0^\circ$, for
 20 tests with different confining pressures. Figure 6 represents the variation of Mode-I

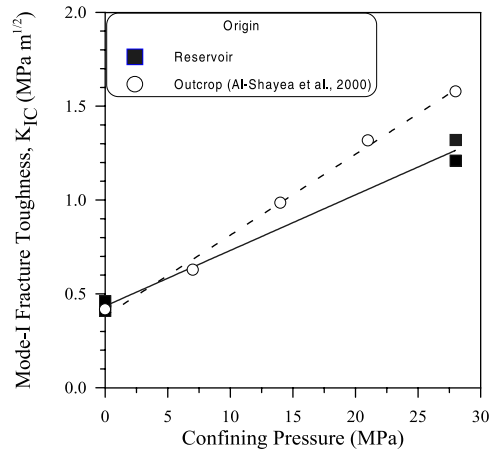


Fig. 6. Variation of Mode-I fracture toughness under confining pressure

1 fracture toughness (K_{IC}) with confining pressure (σ_3). For reservoir specimens,
 2 K_{IC} increased from about 0.41 MPa m^{1/2} at ambient conditions to about 1.32
 3 MPa m^{1/2} under a confining pressure of 28 MPa, representing an increase of
 4 222%. The variation of K_{IC} with σ_3 for reservoir specimens had the following
 5 form:

$$6 \quad K_{IC(\sigma_3)} = K_{IC} + 0.030 * \sigma_3, \quad \text{with } R^2 = 0.990, \quad (5)$$

7 where:

8 σ_3 = effective confining pressure (MPa);
 9 $K_{IC(\sigma_3)}$ = pure Mode-I fracture toughness (MPa m^{1/2}) under any confining pressure σ_3 ; and,
 10 K_{IC} = pure mode-I fracture toughness (MPa m^{1/2}) under ambient conditions.

11 As a comparison, K_{IC} for the outcrop specimens increased from 0.42 MPa m^{1/2}
 12 at ambient conditions to 1.57 MPa m^{1/2} under a confining pressure of 28 MPa
 13 (4000 psi), representing an increase of 274%, Al-Shayea et al. (2000). The variation
 14 of K_{IC} with σ_3 for outcrop specimens were reported to be:

$$15 \quad K_{IC(\sigma_3)} = K_{IC} + 0.043 * \sigma_3, \quad \text{with } R^2 = 0.99. \quad (6)$$

16 Also, Schmidt and Huddle (1977) conducted fracture toughness testing of Indi-
 17 ana limestone under Mode-I conditions using a single edge notched beam in direct
 18 tension. They found a significant increase in the fracture toughness value with
 19 increasing confining pressure. Abou-Sayed (1978) and Muller (1986) reported a
 20 similar trend of fracture toughness variation with confining pressure. Vasarhelyi
 21 (1997), studied the fracture toughness behavior of an anisotropic gneiss using a
 22 single edge cracked beam under a three point bend configuration and reported
 23 similar conclusions. Figure 7 shows a comparison of the Mode-I fracture tough-
 24 ness of various limestone rocks as a function of confining pressure.

25 It is believed that rock behaves in a more ductile manner under triaxial
 26 loading at high confining pressure than at low or no confining pressure conditions.

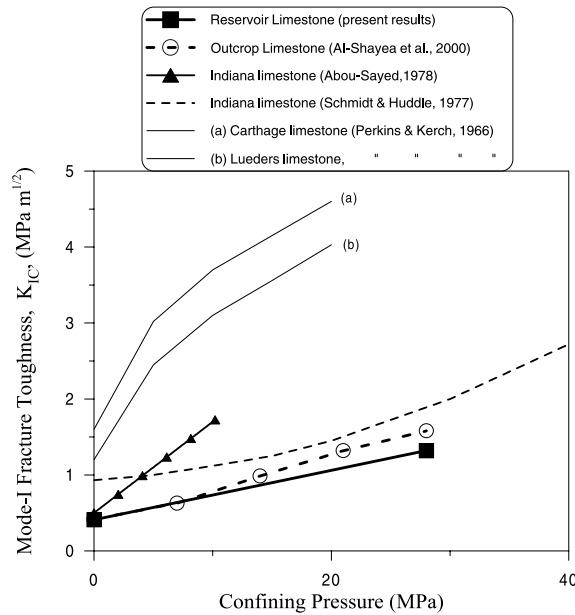


Fig. 7. Influence of confining pressure on Mode-I fracture toughness of various limestone rocks [adapted after Whittaker, et al. (1992)]

1 Increased fracture toughness at high confining pressures has been attributed to the
 2 relatively increased amount of energy required to create new surfaces in ductile
 3 materials. Moreover, confining pressure (a hydrostatic pressure applied to the en-
 4 tire specimen excluding the sealed notch) places the entire specimen under hydro-
 5 static compression. The hydrostatic compression produces an initial negative stress
 6 intensity factor at the crack tip (crack closing), causing an increase in the fracture
 7 toughness value when the load is applied. This effect increases with increasing
 8 confining pressure. Furthermore, an increase in confining pressure reduces the size
 9 of the FPZ.

10

6.3.2 Mixed Mode I–II

11 Mixed Mode I–II fracture toughness results for the reservoir specimens were cal-
 12 culated using Eqs. (1) to (4), given in Table 1, and plotted in Figure 8 for confining
 13 pressures of 0 and 28 MPa (4000 psi). For $\sigma_3 = 28$ MPa, the pure Mode-I fracture
 14 toughness (K_{IC}) was 1.32 MPa m^{1/2}, and the pure the Mode-II fracture toughness
 15 (K_{IIC}) was found to be 2.18 MPa m^{1/2}, which was achieved at a crack inclination
 16 angle of about 29°. Corresponding values of 0.41 and 0.5 MPa m^{1/2} were obtained
 17 at ambient conditions. The mixed Mode I–II fracture toughness results were
 18 compared with those obtained at ambient conditions, and their variations due to
 19 the testing environment can be seen in Fig. 8. A large increase in both Mode-I and
 20 Mode-II fracture toughness values was observed compared to the ambient con-

Table 1. Fracture toughness (K_I and K_{II}) as a function of angle (β)

Testing condition Rock origin	β	Ambient		$\sigma_3 = 28$ MPa		$T = 116^\circ\text{C}$		
		K_I	K_{II}	K_I	K_{II}	K_I	K_{II}	
Reservoir	0	0.410	0.000	1.318	0.000			
	15	0.193	0.304	0.944	1.475			
	27	0.032	0.429	-0.069	2.500			
	30	-0.013	0.428	-1.269	2.291			
	45	-0.355	0.633	-1.963	1.444			
	60	-0.777	0.570	-3.019	0.875			
	75	-1.056	0.306	1.385	0.000			
	0	0.405	0.000	0.963	1.516			
	15	0.181	0.284	-0.068	2.414			
	30	-0.017	0.593	-1.182	2.139			
	60	-0.712	0.523	-2.047	1.522			
	75	-	-	-2.936	0.855			
	Outcrop	0	0.427	0.000	1.579	0.000	0.541	0.000
		15	0.303	0.471	1.039	1.607	0.433	0.670
27		0.077	0.972	-	-	-	-	
30		-0.026	1.063	-0.056	2.355	-0.025	1.049	
45		-0.599	1.095	-1.320	2.419	-0.613	1.124	
60		-1.070	0.802	-2.271	1.711	-1.259	0.947	
75		-1.259	0.377	-3.355	1.010	-1.773	0.534	
0		0.405	0.000	1.376	0.000	0.516	0.000	
15		0.278	0.431	0.898	1.387	0.376	0.580	
27		0.070	0.884	-	-	-	-	
30		-0.024	0.973	-0.056	2.253	-0.026	1.092	
45		-0.573	1.047	-1.253	2.296	-0.598	1.097	
60		-1.156	0.866	-2.082	1.566	-1.231	0.927	
75		-1.358	0.406	-3.145	0.949	-1.983	0.598	

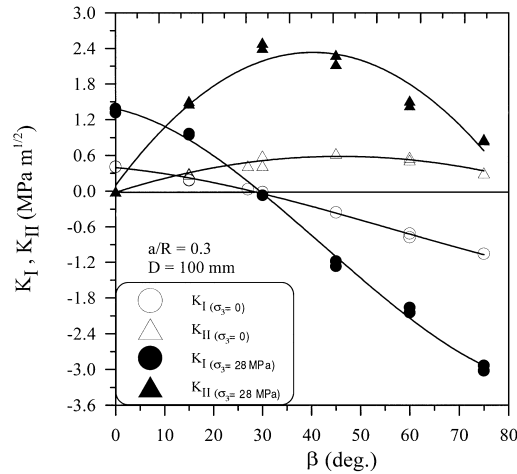


Fig. 8. Comparison of mixed Mode I–II fracture toughness at ambient and confined conditions, for reservoir specimens

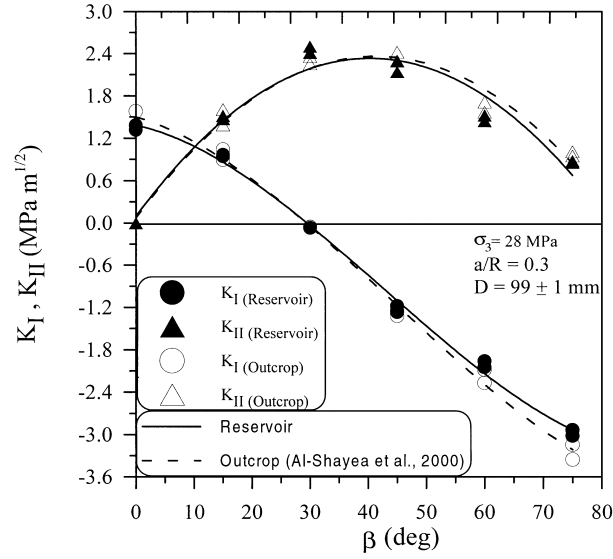


Fig. 9. Comparison of mixed Mode I–II fracture toughness variation for outcrop and reservoir SNBD specimens, under confining pressure

1 ditions. Pure Mode-I and Mode-II fracture toughness values for the specimens
 2 tested under reservoir confining pressure increased by 222% and 336% respec-
 3 tively. The ratio of pure Mode-II to pure Mode-I (K_{IIc}/K_{Ic}) under $\sigma_3 = 28$ MPa
 4 was found to be 1.65 compared to 1.22 at ambient conditions, representing an in-
 5 crease of 35%.

6 As a comparison, results reported by Al-Shayea et al. (2000) indicated that for
 7 the outcrop specimens under $\sigma_3 = 0$ MPa, $K_{Ic} = 0.42$ MPa m^{1/2} and $K_{IIc} = 0.92$
 8 MPa m^{1/2}. The pure Mode-I and Mode-II fracture toughness for confined speci-
 9 mens increased by an amount of 274% and 137%, respectively, over those obtained
 10 under ambient conditions (Table 1). This means that Mode-I fracture toughness
 11 is more affected by the confining pressure than the Mode-II component. The ratio
 12 of pure Mode-II to pure Mode-I (K_{IIc}/K_{Ic}) was 1.39 for the confined specimens,
 13 compared to a value of 2.19 for the unconfined specimens, representing a 37% re-
 14 duction. This is opposite to the 35% increase in the case of reservoir specimens.
 15 This indicates that confining pressure increased K_{IIc} for reservoir specimens more
 16 than that of outcrop specimens. Mixed Mode I–II fracture results for the reservoir
 17 and the outcrop specimens under a σ_3 of 28 MPa are compared in Fig. 9.

18 The normalized fracture toughness for reservoir specimens at a confining pres-
 19 sure of 28 MPa is shown in Fig. 10 to be related to those of the ambient condi-
 20 tions according to the following formula:

$$21 \quad \left(\frac{K_I}{K_{Ic}} \right)_{\sigma_3=28 \text{ MPa}} = 0.941 * \left(\frac{K_I}{K_{Ic}} \right) + 0.109, \quad \text{with } R^2 = 0.984, \quad (7a)$$

$$22 \quad \left(\frac{K_{II}}{K_{IIc}} \right)_{\sigma_3=28 \text{ MPa}} = 0.637 * \left(\frac{K_{II}}{K_{IIc}} \right) + 0.079, \quad \text{with } R^2 = 0.749. \quad (7b)$$

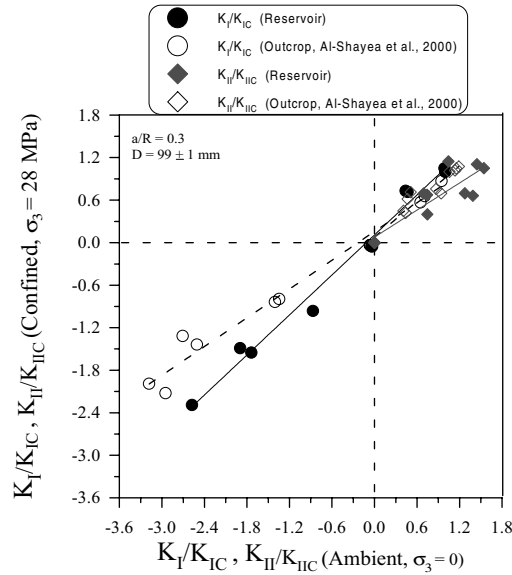


Fig. 10. Comparison of normalized fracture toughness for Mode-I and Mode-II, at ambient and confining pressure, for outcrop and reservoir specimens

6.3.3 Comparison of Results for Outcrop and Reservoir Specimens

To investigate whether the outcrop specimens could be used to determine the *in-situ* fracture behavior of the reservoir rock, results are compared for the mixed Mode I–II fracture toughness results for reservoir and outcrop specimens tested under simulated reservoir conditions of confining pressure. The results of this study for reservoir specimens are compared with those from Al-Shayea et al. (2000) for outcrop specimens. Although specimens from both origins (outcrop and reservoir) showed remarkably different results at ambient conditions (Fig. 5), the results at $\sigma_3 = 28$ MPa for outcrop and reservoir specimens were in extremely good agreement (Fig. 9). When specimens are tested under simulated pressure conditions, the microcracks in the reservoir specimens tend to close due to high confining pressure. Due to this closure of microcracks, specimens become stronger and, hence, a higher fracture toughness was observed.

Figure 11 shows the variation of normalized Mode-I and Mode-II fracture toughness values for the outcrop and reservoir specimens versus those of the outcrop specimens. At ambient conditions, they are related by the following relationships:

$$\left(\frac{K_I}{K_{IC}}\right)_{\text{Reservoir}} = 0.768 \left(\frac{K_I}{K_{IC}}\right)_{\text{Outcrop}}, \quad \text{with } R^2 = 0.976 \quad (8a)$$

$$\left(\frac{K_{II}}{K_{IIC}}\right)_{\text{Reservoir}} = 1.250 \left(\frac{K_{II}}{K_{IIC}}\right)_{\text{Outcrop}}, \quad \text{with } R^2 = 0.964. \quad (8b)$$

Under $\sigma_3 = 28$ MPa, the following relationships were obtained:

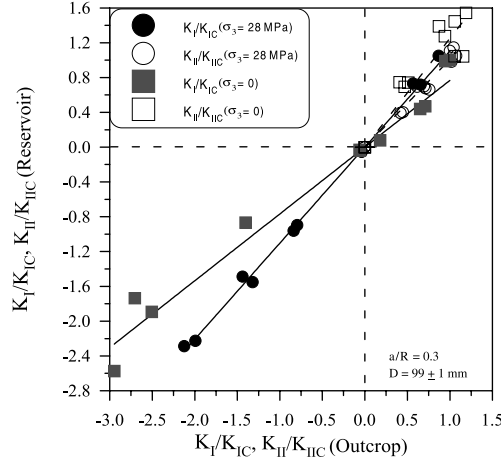


Fig. 11. Comparison of normalized Mode-I and Mode-II fracture toughness for outcrop and reservoir SNBD specimens, at ambient and confined conditions

$$\left(\frac{K_I}{K_{IC}}\right)_{\text{Reservoir}} = 1.100 \left(\frac{K_I}{K_{IC}}\right)_{\text{Outcrop}}, \quad \text{with } R^2 = 0.996 \quad (9a)$$

$$\left(\frac{K_{II}}{K_{IIC}}\right)_{\text{Reservoir}} = 1.011 \left(\frac{K_{II}}{K_{IIC}}\right)_{\text{Outcrop}}, \quad \text{with } R^2 = 0.994. \quad (9b)$$

It is clear, from Eq. (9), that at reservoir conditions of high pressure, the normalized fracture toughness of the reservoir and outcrop specimens are very close to each other.

6.4 Temperature

6.4.1 Mode-I

The Mode-I fracture toughness was found by using Eqs. (1) and (3), and its variation with temperature is shown in Fig. 12. A small increase in the pure Mode-I (K_{IC}) fracture toughness value was observed, from a value of $0.41 \text{ MPa m}^{1/2}$ for reservoir specimens at ambient conditions to $0.51 \text{ MPa m}^{1/2}$ at 116°C . The fracture toughness for reservoir specimens, at a typical reservoir temperature (i.e., 116°C), was 24% higher than the value obtained at ambient conditions. Similar increase was reported for outcrop specimens, Al-Shayea et al. (2000). Predictably, K_{IC} may decrease at much higher temperatures due to thermal expansion. For the reservoir specimens, the variation of K_{IC} with temperature, T , ($K_{IC(T)}$) had the following forms:

$$K_{IC(T)} = K_{IC} + 1.1 \times 10^{-3} * (T - 27). \quad (10)$$

Similar findings have also been reported in the literature although various testing methods other than the notched Brazilian disks were used in those investigations. For outcrop specimens, Al-Shayea et al. (2000) obtained a formula

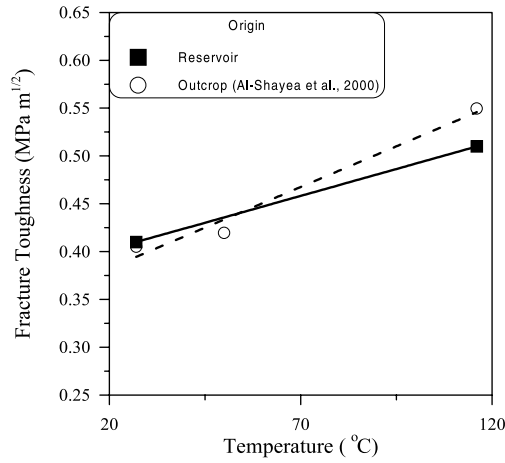


Fig. 12. Effect of temperature on Mode-I fracture toughness of outcrop and reservoir SNBD specimens

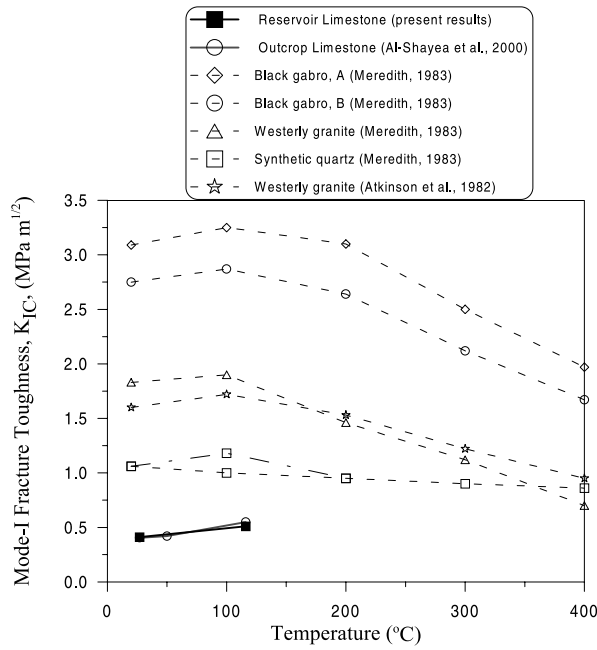


Fig. 13. Effect of temperature on Mode-I fracture toughness of various rocks [adapted after Whittaker, et al. (1992)]

- 1 similar to the above equation. Whittaker et al. (1992) summarized these findings,
- 2 and mentioned that the fracture toughness variation with temperature is material
- 3 dependent, and concluded that the fracture toughness for rocks generally increases
- 4 slightly at low temperatures (20°C–100°C). Figure 13 shows comparisons of
- 5 Mode-I fracture toughness for various rocks as a function of temperature.

6.4.2 Mode II

The pure Mode II fracture toughness was calculated using Eqs. (2) and (4). For reservoir specimens, pure Mode-II (K_{IIc}) was found to be 0.56 MPa m^{1/2} compared to 0.50 MPa m^{1/2} at ambient condition. The ratio of pure Mode-II and pure Mode-I (K_{IIc}/K_{Ic}) was 1.10 as compared to a value of 1.22 at ambient conditions.

6.5 Comparing Results at Ambient and In-Situ Conditions

Table 2 gives a summary of K_{Ic} , K_{IIc} , and K_{IIc}/K_{Ic} for reservoir and outcrop specimens, at different conditions (ambient, $\sigma_3 = 28$ MPa, and $T = 116^\circ\text{C}$). The ratios of K_{Ic} , K_{IIc} and K_{IIc}/K_{Ic} of the reservoir specimens to the corresponding values for outcrop specimens are 0.98, 0.54, and 0.56 at ambient conditions; 0.84, 1.00, and 1.19 at $\sigma_3 = 28$ MPa; and 0.98, 0.56, and 0.57 at $T = 116^\circ\text{C}$. The ratios of K_{Ic} , K_{IIc} , and K_{IIc}/K_{Ic} at $\sigma_3 = 28$ MPa to the corresponding values at ambient conditions are 3.22, 4.36, and 1.35 for reservoir specimens, as compared to 3.74, 2.37, and 0.63 for outcrop specimens. Also, the ratios of K_{Ic} , K_{IIc} , and K_{IIc}/K_{Ic} at $T = 116^\circ\text{C}$ to the corresponding values at ambient conditions are 1.24, 1.12, and 0.90 for reservoir specimens, as compared to 1.24, 1.09, 0.88 for outcrop specimens. Therefore, the effects of confining pressure and temperature are much more pronounced on K_{IIc} for reservoir specimens.

Using simple superposition of the individual effects of confining pressure and temperature, the combined effect of *in-situ* temperature and confining pressure on Mode-I fracture toughness in the field (Eqs. 5 and 10), $K_{Ic(\text{field})}$, can be written as follows:

$$K_{Ic(\text{field})} = K_{Ic} + 0.03 * \sigma_3 + 1.1 \times 10^{-3}(T - 27). \quad (11)$$

This equation forms a base for the estimation of the in-situ fracture toughness in the reservoir, $K_{Ic(\text{field})}$, (for the reservoir rocks, at the reservoir condition) using outcrop specimens from the same geological formation. This correlation will solve

Table 2. Comparison between K_{Ic} , K_{IIc} , and their ratio for outcrop and reservoir SNBD specimens at ambient and in-situ conditions

Condition	Origin	K_{Ic} (MPa m ^{1/2})	K_{IIc} (MPa m ^{1/2})	K_{IIc}/K_{Ic}
Ambient	Reservoir	0.41	0.50	1.22
	Outcrop	0.42	0.92	2.19
	Reservoir/Outcrop	0.98	0.54	0.56
$\sigma_3 = 28$ MPa	Reservoir	1.32	2.18	1.65
	Outcrop	1.57	2.18	1.39
	Reservoir/Outcrop	0.84	1.00	1.19
$T = 116^\circ\text{C}$	Reservoir	0.51	0.56	1.10
	Outcrop	0.52	1.00	1.92
	Reservoir/Outcrop	0.98	0.56	0.57
Ratio at ($\sigma_3 = 28$ MPa) to (ambient)	Reservoir	3.22	4.36	1.35
	Outcrop	3.74	2.37	0.63
Ratio at ($T = 116^\circ\text{C}$) to (ambient)	Reservoir	1.24	1.12	0.90
	Outcrop	1.24	1.09	0.88

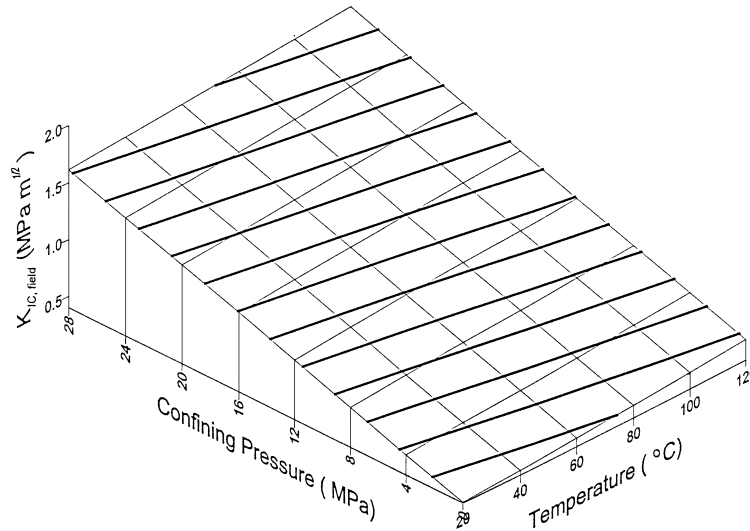


Fig. 14. Combined effect of temperature and confining pressure on Mode I fracture toughness, of reservoir specimens

1 the problem of the limited availability of reservoir rock samples and it will increase
 2 the confidence by obtaining more data when testing many samples from the less
 3 expensive outcrop rock. It will also reduce the testing cost by reducing the cost of
 4 the rock material. Eq. (11), with $K_{IC} = 0.41$, is presented as a 3-D plot in Fig. 14.

6.6 Fracture Toughness Envelope

6 The normalized fracture toughness values of (K_I/K_{IC}) and (K_{II}/K_{IIC}) were deter-
 7 mined for reservoir specimens at various conditions. The plot of (K_{II}/K_{IIC}) vs.
 8 (K_I/K_{IC}) is known as the fracture toughness envelope, which is the fracture locus
 9 for the general Mixed-Mode I–II loading. Crack initiates when a point $(K_I/K_{IC},$
 10 $K_{II}/K_{IIC})$ falls on the envelope. Figure 15 gives a comparison between fracture
 11 toughness envelopes at different conditions (ambient and $\sigma_3 = 28$ MPa) at both
 12 positive region (crack opening) and negative region (crack closing). A second-
 13 degree polynomial was used to fit the experimental data at various conditions, and
 14 at both positive and negative region, Fig. 15. The general form suggested for this
 15 fitting is:

$$(K_{II}/K_{IIC}) = A + B(K_I/K_{IC}) + C(K_I/K_{IC})^2 \quad (12)$$

17 where, A , B , and C are the coefficient for the second order polynomial used for
 18 the regression. The values of A , B , and C for various experimental conditions are
 19 tabulated in Table 3.

20 It can be seen from Fig. 15 that the fracture toughness envelope cannot be
 21 approximated by the famous simple empirical equations of straight line, ellipse,
 22 or homogenous quadratic, especially in the negative region. Fracture toughness

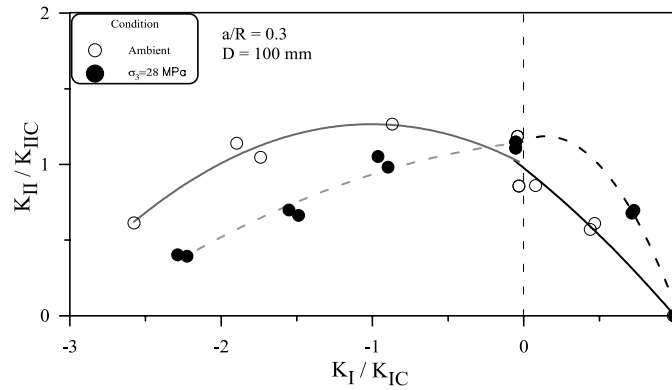


Fig. 15. Fracture toughness envelopes for SNBD reservoir specimens

Table 3. Regression parameters for various fracture toughness envelopes of reservoir specimens

Condition	Region	A	B	C	R^2
Ambient	Positive	0.9759	-0.7964	-0.1824	0.949 & 0.951
	Negative	1.0013	-0.5265	-0.2618	0.184 & 0.778
$\sigma_3 = 28$ MPa	Positive	1.1545	0.4396	-1.5225	0.865 & 0.991
	Negative	1.1468	0.1120	-0.1010	0.925 & 0.964

1 envelop at high confining pressure switched its behavior from being higher than
 2 that at ambient condition in the positive region to be lower in the negative region.
 3 Some values of K_{II}/K_{IIC} exceeded 1 in the negative region, because the values of
 4 K_{IIC} were taken from the curves fitting the data in Fig. 8.

5

7. Conclusions

6 It is essential to determine the fracture toughness of rocks in the temperature and
 7 confining pressure ranges of operation. Testing under such conditions requires
 8 the development of an apparatus that can simulate *in-situ* conditions. Some conclusions
 9 pertaining to the investigated limestone rocks from the Khuff formation,
 10 Saudi Arabia are drawn below.

11 The SNBD type was found to be the most convenient geometry to use for
 12 the determination of pure Mode-I, pure Mode-II, and mixed Mode I–II fracture
 13 toughness of rocks. This made it possible after successfully machining a straight
 14 notch inside the disk, and using the combination of a drill and a wire saw to make
 15 a precise notch.

16 Despite the fact that the fracture toughness values of the reservoir and the
 17 outcrop specimens from the same formation were significantly different at ambient
 18 conditions (Fig. 5), their values under confining pressure were very well matched
 19 (Fig. 9). It is therefore concluded that the behavior of reservoir rocks can be suc-
 20 cessively determined by testing outcrop specimens under simulated reservoir con-
 21 ditions, as suggested by Eq. (11).

1 Comparisons of Eqs. (5) and (10) with those corresponding to outcrop speci-
 2 mens indicate that K_{IC} of reservoir specimens are less affected by confining pres-
 3 sure and temperature, relative to that of outcrop specimens.

4 The Mode-I fracture toughness (K_{IC}) was found to increase substantially with
 5 increased confining pressure. This increase is almost linear in the pressure range
 6 from 0 to 28 MPa. At $\sigma_3 = 28$ MPa, K_{IC} increased by 222% for reservoir speci-
 7 mens and by 274% for outcrop specimens, with respect to the corresponding
 8 values of ambient conditions. However, at $T = 116^\circ\text{C}$, K_{IC} increased only slightly
 9 by 24% for both reservoir and outcrop specimens.

10 The Mode-II fracture toughness (K_{IIC}) was also found to increase with in-
 11 creased confining pressure. At $\sigma_3 = 28$ MPa, K_{IIC} increased by 336% for reservoir
 12 specimens, as compared to only by 137% for outcrop specimens. However, at
 13 $T = 116^\circ\text{C}$, K_{IIC} increased only by 12% for reservoir specimens and by 9% for
 14 outcrop specimens.

15 For reservoir specimens, the increase of K_{IIC} due to confining pressure (336%)
 16 is more than that of K_{IC} (222%) while the increase of K_{IIC} (12%) is less than that of
 17 K_{IC} (24%). The ratio of K_{IIC}/K_{IC} was equal to 1.22, 1.65, and 1.10 at ambient
 18 conditions, under $\sigma_3 = 28$ MPa, and at $T = 116^\circ\text{C}$, respectively.

19 The above observations indicate that the Mode-II component may be the most
 20 critical mode controlling failure at high values of temperature and confining pres-
 21 sure. Also, the effect of confining pressure on K_{IC} and K_{IIC} is much more signifi-
 22 cant than the effect of temperature.

23 The fracture toughness envelope is suggested to have a form of second-order
 24 polynomial (Eq. 12). This form is general and can be used for both positive and
 25 negative regions.

26 Acknowledgements

27 The author acknowledges the support of King Fahd University of Petroleum and Minerals
 28 for providing computing and laboratory facilities. He also would like to acknowledge the
 29 support of Saudi-ARAMCO via the Research Institute, KFUPM. He is also grateful for the
 30 assistance of Mr. Khaqan Khan and Dr. Abdurraheem from the Center of Petroleum
 31 Engineering and Mr. Hasan Zakaria from the Geotechnical Laboratory.

32 References

- 33 Abe, H., Keer, L. M., Mura, T. (1979): Theoretical study of hydraulic fractured penny-
 34 shaped cracks in hot, dry rocks. *Int. J. Numer. Anal. Meth. Geomech.* 3, 79–96.
- 35 Abou-Sayed, A. S. (1978): An experimental technique for measuring the fracture toughness
 36 of rocks under downhole stress condition. *VDI-Berichte No. 313*, 819–824.
- 37 Al-Jalal, A. I. (1994): The Khuff formation: its reservoir potential in Saudi Arabia and
 38 other Gulf countries; Depositional and stratigraphic approach. In: Al-Husseini, M. I.
 39 (ed.) *GEO '94, The Middle East Petroleum Geosciences Conference*, April 25–27, 1994,
 40 Bahrain. Gulf PetroLink, Manamah, Bahrain, 103–119.
- 41 Al-Shayea, N. A., Khan, K., Abduljauwad, S. N. (2000): Effects of confining pressure and
 42 temperature on mixed-mode (I–II) fracture toughness of a limestone rock formation.
 43 *Int. J. Rock Mech. Min. Sci.* 37(4), 629–643.

- 1 Atkinson, C., Smelser, R. E., Sanchez, J. (1982): Combined mode fracture via the cracked
2 brazilian disk. *Int. J. Fracture* 18, 279–291.
- 3 ASTM Standards (1993): Soil and rocks. *Annual Book of ASTM Standards*, Vol. 4.08.
- 4 Awaji, H., Sato, S. (1978): Combined mode fracture toughness measurement by the disk
5 test. *J. Engng. Mater. Technol.* 100, 175–182.
- 6 Barton, C. C. (1982): Variables in fracture energy and toughness testing of rock. *Proc.*, 23rd
7 U.S. Symposium on Rock Mechanics, 145–157.
- 8 Fowell, R. J., Xu, C. (1994): The use of the cracked brazilian disk geometry for rock frac-
9 ture investigations. *Int. J. Rock Mech. Min. Sci. Geomech. Abstr.* 31(6), 571–579.
- 10 Hoagland, R. G., Hahn, G. T., Rosenfield, A. R. (1973): Influence of microstructure on
11 fracture propagation in rock. *Rock Mech.* 5, 77–106.
- 12 Huang, J., Wang, S. (1985): An experimental investigation concerning the comprehensive
13 fracture toughness of some brittle rocks. *Int. J. Rock Mech. Min. Sci. Geomech. Abstr.*
14 22(2), 99–104.
- 15 Khan, K., Al-Shayea, N. A. (2000): Effect of specimen geometry and testing methods on
16 mixed-mode II fracture toughness of a limestone rock from Saudi Arabia. *Rock Mech.*
17 *Rock Engng.* 33(3), 179–206.
- 18 Krishnan, G. R., Zhao, X. L., Zaman, M., Rogiers, J. C. (1998): Fracture toughness of a
19 soft sandstone. *Int. J. Rock Mech.* 35, 195–218.
- 20 Lim, I. L., Johnston, I. W., Choi, S. K. (1994a), Assessment of mixed mode fracture
21 toughness testing methods for rock. *Int. J. Rock Mech. Min. Sci. Geomech. Abstr.*
22 31(3), 265–272.
- 23 Lim, I. L., Johnston, I. W., Choi, S. K., Boland, J. N. (1994b): Fracture testing of a soft
24 rock with semicircular specimens under three point bending, Part 1. *Int. J. Rock Mech.*
25 *Min. Sci. Geomech. Abstr.* 31(3), 185–197.
- 26 Meredith, P. G. (1983): A fracture mechanics study of experimentally deformed crystal
27 rocks. PhD. Thesis, University of London.
- 28 Mitchell, J. K. (1993): *Fundamentals of soil behavior*, 2nd edn. John Wiley, New York, 437.
- 29 Muller, W. (1986): Brittle crack growth in rock. *PAGEOPH* 124(4/5), 694–709.
- 30 Perkins, T. K., Krech, W. W. (1966): Effect of cleavage rate and stress level on apparent
31 surface energies of rocks. *Soc. Petrol. Engineers J.* ■ 308–314.
- 32 Powers, L. F., Ramirez, L. F., Redmond, C. D., Elberg Jr., E. L. (1963): *Geology of the*
33 *Arabian peninsula-sedimentary geology of Saudi Arabia*. ARAMCO-USGS, 147 p.
- 34 Rummel, F., Winter, R. B. (1982): Application of laboratory fracture mechanics data to
35 hydraulic fracturing field tests. *Proc.*, 1st Japan-USA Symp. on Fracture Mechanics
36 Approach, Hydraulic Fracture and Geothermal Energy, Sendai, Japan, 495–501.
- 37 Sanchez, J. (1979): Application of the disk test to mode-I–II fracture toughness analysis.
38 M.S. Thesis, Department of Mechanical Engineering, University of Pittsburgh, U.S.A.
- 39 Schmidt, R. A. (1976): Fracture-toughness testing of limestone. *Exp. Mech.* 16, 161–167.
- 40 Schmidt, R. A., Huddle, C. W. (1977): Effect of confining pressure on fracture toughness of
41 Indiana limestone. *Int. J. Rock Mech. Min. Sci. Geomech. Abstr.* 14, 289–293.
- 42 Shetty, D. K., Rosenfield, A. R., Duckworth, W. H. (1986): Mixed mode fracture of ce-
43 ramic in diametral compression. *J. Am. Ceram. Soc.* 69, 437–443.
- 44 Shlyapobersky, J. (1985): Energy analysis of hydraulic fracturing. *Proc.*, 26th U.S. Symp. on
45 Rock Mech., Rapid City, SD, 539–548.

- 1 Sih, G. C., Liebowitz, H. (1968): Mathematical theories of brittle fracture. In: Fracture, –
2 an advanced treatise, Vol. II. Academic Press, New York, 68–190.
- 3 Sun, G. X. (1990): Application of fracture mechanics to mine design. PhD Thesis, Dept. of
4 Mining Engineering University, Nottingham, England.
- 5 Thallak, S., Holder, J., Gray, K. E. (1993): The pressure dependence of apparent hydro-
6 fracture toughness. *Int. J. Rock Mech. Min. Sci. Geomech. Abstr.* 30(7), 831–835.
- 7 Vasarhelyi, B. (1997): Influence of pressure on the crack propagation under mode-I loading
8 in anisotropic gneiss. *Rock Mech. Rock Engng.* 30(1), 59–64.
- 9 Whittaker, B. N., Singh, R. N., Sun, G. (1992): Rock fracture mechanics; principles, design
10 and applications. *Developments in Geotechnical Engineering*, Elsevier, Amsterdam.
- 11 **Author's address:** Dr. Naser A. Al-Shayea, Associate Professor, Civil Engineering De-
12 partment, King Fahd University of Petroleum and Minerals, KFUPM Box 368, Dhahran
13 31261, Saudi Arabia; E-mail: nshayea@kfupm.edu.sa

